

# GLASS FORMATION REGION OF THE LITHIUM IRON PHOSPHATE TERNARY SYSTEM AND THE PROPERTIES OF OBTAINED GLASSES

RUIJUAN YANG, YINGHUI WANG, YAMING CHEN, XIAOPENG HAO\*, JIE ZHAN\*, SHIQUAN LIU#

School of Materials Science and Engineering,  
University of Jinan, Jinan 250022, Shandong, China  
\*State Key Laboratory of Crystal Materials,  
Shandong University, Jinan 250100, Shandong, China

#Corresponding author, e-mail: mse\_liusq@ujn.edu.cn

Submitted June 23, 2010; accepted October 26, 2010

**Keywords:** LiFePO<sub>4</sub> glass, Glass formation region, Density, Chemical stability, Crystallization tendency

*The glass formation region of the lithium iron phosphate ternary system was determined with the help of XRD and optical microscope analysis. Nine Li<sub>2</sub>O–Fe<sub>2</sub>O<sub>3</sub>–P<sub>2</sub>O<sub>5</sub> ternary glasses with compositions inside the glass formation region were prepared. Glass transition temperature and crystallization tendency of the glasses were analyzed by DTA. Density and water resistance of the glasses were measured based on the Archimedes principle and the weight loss of the glass particles after being boiled in water, respectively. The results show that the increase in the amount of either Li<sub>2</sub>O or Fe<sub>2</sub>O<sub>3</sub> (decrease of P<sub>2</sub>O<sub>5</sub>) results in the increase in the glass density and the decrease in the glass transformation temperature. The chemical stability of the glasses is increased, while the crystallization tendency is reduced with increased amounts of Fe<sub>2</sub>O<sub>3</sub>. However, glasses with more Li<sub>2</sub>O have a stronger tendency to crystallize and are generally less resistant to water attack.*

## INTRODUCTION

Usable energy has become one of the most concerned issues around the world since the oil crisis. One possible solution is to search for new alternative energy resources. Lithium ion batteries have attracted great interest due to their high specific energy, high voltage and long service life [1]. Significant progress has been made on developing anode and electrolyte materials for use in rechargeable lithium-ion batteries. However, the study and application of cathode materials fall relatively behind. At the present, the main cathode material is LiCoO<sub>2</sub>. However, it suffers from several disadvantages. First, it is unstable and may decompose or even explode when it is overcharged and overheated. Furthermore, the supply of global cobalt resources is limited. In addition, cobalt is harmful to the environment and human beings. Thus, the application of LiCoO<sub>2</sub> in power devices is being challenged. For the further improvement of performance and the cost reduction of lithium ion batteries, new cathode materials have to be developed [2].

Lithium iron phosphate (LiFePO<sub>4</sub>) with the olivine structure has been found to have the capability to extract and reinsert lithium ion reversibly [3]. LiFePO<sub>4</sub> has a high

theoretical capacity and a good cycling performance. It is thermally stable in fully-charged state, environmentally benign and has a low raw materials cost. Lithium iron phosphate materials have great potential as cathode materials for the next generation of rechargeable lithium ion batteries [4-5].

Many different routes have been developed for the preparation of LiFePO<sub>4</sub> cathode materials [6]. Generally, three common steps were involved. First, solid mixing, microwave heating, or the sol-gel method was used to synthesize compound powder precursor. Then the precursor was calcined in a furnace under protective atmosphere so that the synthesized compounds decomposed and reacted to form LiFePO<sub>4</sub>. Finally, the calcined product was cooled and milled and pressed into blocks under given pressures. LiFePO<sub>4</sub> materials prepared with the above steps have relatively low tap densities due to the influence of the particle morphology, size, distribution and the densification of the LiFePO<sub>4</sub> powders.

Recently, Hirose [7] and Garbarczyk *et al.* [8-10] reported a new way to prepare LiFePO<sub>4</sub> electrode material. It was based on the crystallization of LiFePO<sub>4</sub> glasses. Since the glasses are highly dense and the derived glass-ceramics could be analogs of the sintered

LiFePO<sub>4</sub> materials which are obtained via the traditional powder densification method, LiFePO<sub>4</sub> derived glass-ceramics could replace the traditional LiFePO<sub>4</sub> cathodes. Up to now, only a few lithium iron phosphate glasses have been studied. The aim of the present work is to determine the glass formation region of the Li<sub>2</sub>O-Fe<sub>2</sub>O<sub>3</sub>-P<sub>2</sub>O<sub>5</sub> ternary system. Glass transition temperature and crystallization tendency, density and water attack resistance of the glasses with compositions inside the determined glass formation region were measured and compared.

## EXPERIMENTAL

Analytic grade reagents of Li<sub>2</sub>CO<sub>3</sub>, Fe<sub>2</sub>O<sub>3</sub> and NH<sub>4</sub>H<sub>2</sub>PO<sub>4</sub> were used as the raw materials for preparing glass batches. First, batches with Fe<sub>2</sub>O<sub>3</sub>/P<sub>2</sub>O<sub>5</sub> molar ratios of 35:65, 43:57, 45:55, 50:50, 55:45 and a wide range of Li<sub>2</sub>O/Fe<sub>2</sub>O<sub>3</sub>/P<sub>2</sub>O<sub>5</sub> molar ratios were prepared by mixing proportionally weighed raw materials and melted at 1200°C for 1h. The melts were cast in a steel mould and annealed at 350°C for 1h. Powder X-ray diffraction (XRD) analysis was performed on a D8-advanced diffractometer (Bruke, Germany) to check whether the obtained samples were devitrified or not. For the samples which were critical to the determination of the glass formation region, polarized optical microscope analysis was carried out to make sure that there were no crystals below the XRD detection limit.

To investigate the influence of composition on the properties of Li<sub>2</sub>O-Fe<sub>2</sub>O<sub>3</sub>-P<sub>2</sub>O<sub>5</sub> ternary glasses, nine glasses with different compositions inside the determined glass formation region were prepared with the aforementioned procedures. The glass transformation and crystallization temperatures of the glasses were determined using differential thermal analysis (DTA) technology. Sample powders were placed in alumina crucibles and heated with a rate of 5°C per minute to 700°C in a HCT-1 (Henven, China) thermal analyzer with an empty crucible as reference. The densities of glasses were measured based on the Archimedes principle. Glass samples were ground to a size of 425-250 microns and boiled in water for 2 h, followed by filtration and drying in an oven at 120°C overnight. The weights of the sample powders before and after being boiled in water were compared to evaluate the chemical durability of glasses.

## RESULTS AND DISCUSSION

### Glass formation region

It is well known that P<sub>2</sub>O<sub>5</sub> is a glass former. The glass formation region of the Li<sub>2</sub>O-P<sub>2</sub>O<sub>5</sub> binary system has been reported in the literature. As indicated by the point 1 in Figure 1, the binary Li<sub>2</sub>O-P<sub>2</sub>O<sub>5</sub> glasses could

be formed with Li<sub>2</sub>O up to 60 mol.% [11]. Therefore, the key to determine the glass formation region of the Li<sub>2</sub>O-Fe<sub>2</sub>O<sub>3</sub>-P<sub>2</sub>O<sub>5</sub> ternary system lies in the determination of the glass formation region of the Fe<sub>2</sub>O<sub>3</sub>-P<sub>2</sub>O<sub>5</sub> binary system and the boundary line connecting the maximal Li<sub>2</sub>O and Fe<sub>2</sub>O<sub>3</sub> points at which binary Li<sub>2</sub>O-P<sub>2</sub>O<sub>5</sub> and Fe<sub>2</sub>O<sub>3</sub>-P<sub>2</sub>O<sub>5</sub> glasses can be formed.

The XRD patterns of binary Fe<sub>2</sub>O<sub>3</sub>-P<sub>2</sub>O<sub>5</sub> samples with Fe<sub>2</sub>O<sub>3</sub>/P<sub>2</sub>O<sub>5</sub> molar ratios of 35:65, 43:57 and 50:50 are depicted in Figure 2. It can be seen that no diffraction peaks except broad diffraction halos are shown in the patterns (Figure 2a-c), indicating that these samples are amorphous. Polarized optical microscope analysis further ensured these results were accurate. However, the sample with a Fe<sub>2</sub>O<sub>3</sub>/P<sub>2</sub>O<sub>5</sub> molar ratio of 55:45 was found to have many centimeter-sized red stains on the sample surface, and therefore not analyzed by XRD. By further increasing the Fe<sub>2</sub>O<sub>3</sub>/P<sub>2</sub>O<sub>5</sub> ratio (e.g. 75:25), the obtained sample became delaminated and iron-like, showing no features of glass. Crystals were also detected by the XRD analysis. Therefore, it is concluded that the binary Fe<sub>2</sub>O<sub>3</sub>-P<sub>2</sub>O<sub>5</sub> glass can be formed with the amount of Fe<sub>2</sub>O<sub>3</sub> up to 50 mol.%. Microscope observation further identified that the sample with a Fe<sub>2</sub>O<sub>3</sub>/P<sub>2</sub>O<sub>5</sub> molar ratio of 50/50 is amorphous. The results above suggest that the glass formation region in the Fe<sub>2</sub>O<sub>3</sub>-P<sub>2</sub>O<sub>5</sub> binary system is smaller than that in the Li<sub>2</sub>O-P<sub>2</sub>O<sub>5</sub> binary system. The observed experimental phenomenon indicates a low solubility of iron oxide in the binary phosphate system. This could be due to the fact that the electric field strength of Fe<sup>3+</sup> ions is higher than that of Li<sup>+</sup>, which results in a higher precipitation tendency.

To determine the glass formation region of the ternary system, samples with compositions correspondent to the points 2-17 in Figure 1 were prepared and analyzed by the XRD and microscope analysis. During the experiments, it was found that glasses No.2-7 were homogeneous, brittle, fragile and had apparent glass

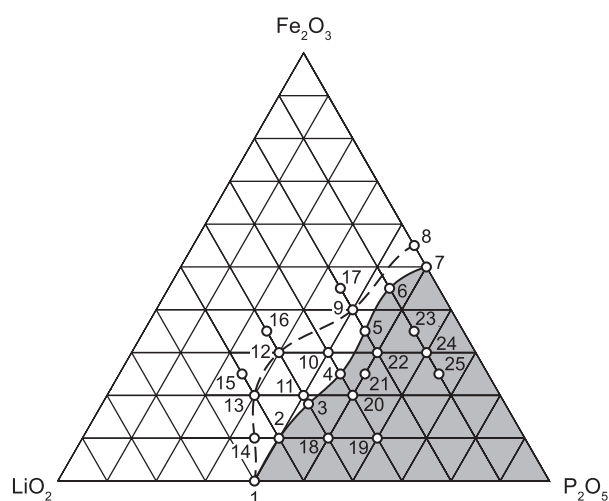


Figure 1. Glass formation region inside the ternary system of Li<sub>2</sub>O-Fe<sub>2</sub>O<sub>3</sub>-P<sub>2</sub>O<sub>5</sub>.

luster. However, the samples with  $\text{Li}_2\text{O}/\text{Fe}_2\text{O}_3/\text{P}_2\text{O}_5$  molar ratios correspondent to the points 8-17 were all delaminated to some extent. The XRD analysis showed that glasses No.2-7 were amorphous (Figure 3). This was further identified by the polarized optical microscope observations.

Based on the above results, the glass formation region of the  $\text{Li}_2\text{O}-\text{Fe}_2\text{O}_3-\text{P}_2\text{O}_5$  ternary system is determined and shown by the shaded area in Figure 1. It was also proved that the water quenched samples with compositions correspondent to the points 8-14 in Figure 1 were also not crystalline, while water quenched samples No. 15-17 were crystalline. Therefore, the glass formation region can be extended to the dash line in Figure 1 if the water quenching instead of the normal casting-annealing procedure is applied.

#### Differential thermal analysis

The DTA curves of the glasses with compositions inside the glass formation region are shown in Figure 4. It can be seen from Figure 4a that when the amount of  $\text{Fe}_2\text{O}_3$  is fixed at 10 mol%, the glass transformation temperature ( $T_g$ ) decreases from 372°C to 361°C as  $\text{P}_2\text{O}_5$  is replaced by  $\text{Li}_2\text{O}$  (points 19→18→2). The decrease in the  $T_g$  temperature with the addition of  $\text{Li}_2\text{O}$  is indicative of the decrease in the viscosity of glass, which can be ascribed to the increase in non-bridging oxygens due to the cleavage of P–O–P bonds to form P–O–Li<sup>+</sup> bonds. In addition, the high mobility of Li<sup>+</sup> also contributes to the decrease in the viscosity of glass. A more significant difference lies in the crystallization behavior of glasses

with different  $\text{P}_2\text{O}_5$  and  $\text{Li}_2\text{O}$  contents. A broad crystallization peak at 651°C is observed for the sample with 30 mol%  $\text{Li}_2\text{O}$  (point 19). The DTA curves of glasses No.18 and 2 (Figure 4b and c) show profoundly obvious exothermal crystallization peaks. The crystallization peak temperature ( $T_c$ ), decreases from 548°C to 461°C with the increase of  $\text{Li}_2\text{O}$ , indicating that the glasses with more  $\text{Li}_2\text{O}$  have a stronger tendency to crystallize. However, for both glasses No.18 and 2, a second exothermal peak appears, accompanied by a small endothermal peak ahead of them. It may suggest the melting of pre-formed first crystals and a recrystallization process. Figure 4b shows that the  $T_g$  temperature of the glasses with a fixed amount of 10 mol%  $\text{Li}_2\text{O}$  decreases from 488 to 471°C when  $\text{P}_2\text{O}_5$  is replaced by  $\text{Fe}_2\text{O}_3$  (points 25→24→23). However, in contrast to the crystallization behavior of glasses with increasing amounts of  $\text{Li}_2\text{O}$ , glasses with more  $\text{Fe}_2\text{O}_3$  have a weaker tendency to crystallize, indicated by the broadening of exothermal peak and the increase in the  $T_c$  temperature. The result suggests  $\text{Fe}_2\text{O}_3$  behaves like a network former, cross-linking some 2D chains in the phosphate glasses. Therefore, the decrease in the viscosity of glass as indicated by the decrease in the  $T_g$  temperature is related to the high polarizability of Fe ions. For the glass containing the highest amount of  $\text{Fe}_2\text{O}_3$  (No. 23), no crystallization peak is observed. If  $\text{P}_2\text{O}_5$  is fixed at 50 mol.%, glasses with different  $\text{Li}_2\text{O}/\text{Fe}_2\text{O}_3$  ratios of 20:30, 25:25 and 30:20 depict DTA curves each with two connected crystallization peaks (Figure 4c). Both  $T_g$  and  $T_c$  are rising when more  $\text{Li}_2\text{O}$  is replaced by  $\text{Fe}_2\text{O}_3$  (No.20→22). Details have to be investigated further.

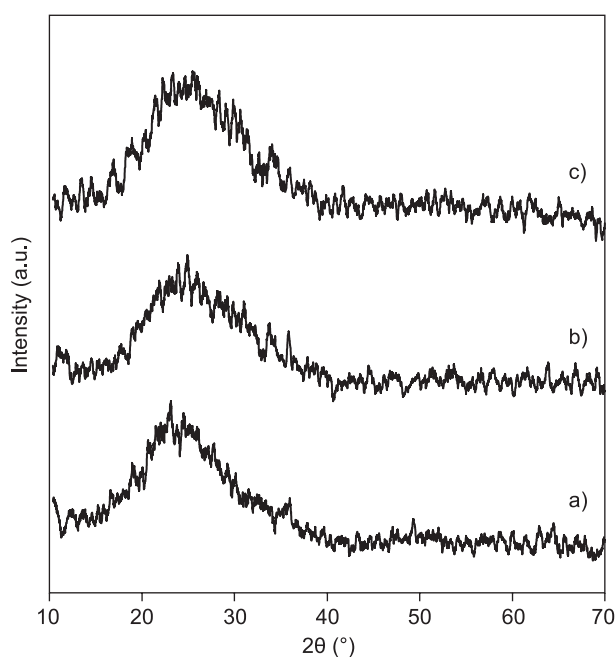


Figure 2. XRD patterns of binary  $\text{Fe}_2\text{O}_3-\text{P}_2\text{O}_5$  glasses with  $\text{Fe}_2\text{O}_3/\text{P}_2\text{O}_5$  molar ratios of a) 35:65, b) 43:55, c) 50:50.

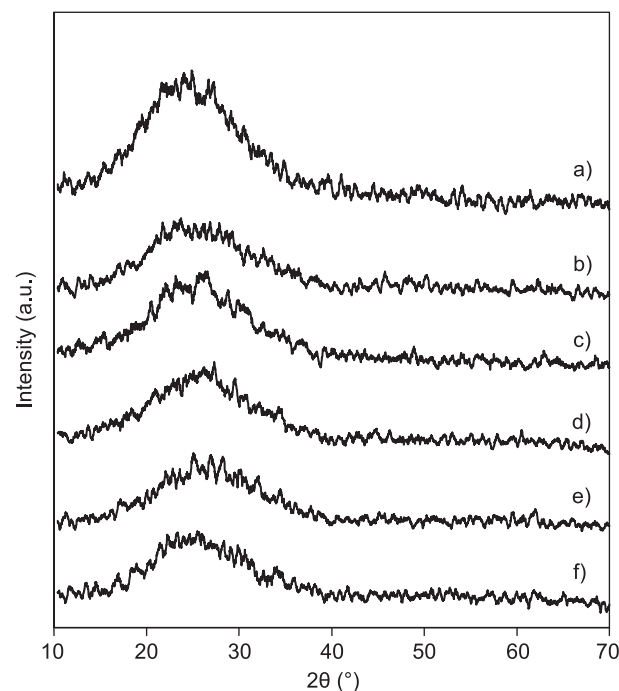


Figure 3. XRD patterns of ternary  $\text{Li}_2\text{O}-\text{Fe}_2\text{O}_3-\text{P}_2\text{O}_5$  glasses with  $\text{Li}_2\text{O}/\text{Fe}_2\text{O}_3/\text{P}_2\text{O}_5$  molar ratios correspondent to the points: a) 2, b) 3, c) 4, d) 5, e) 6, f) 7.

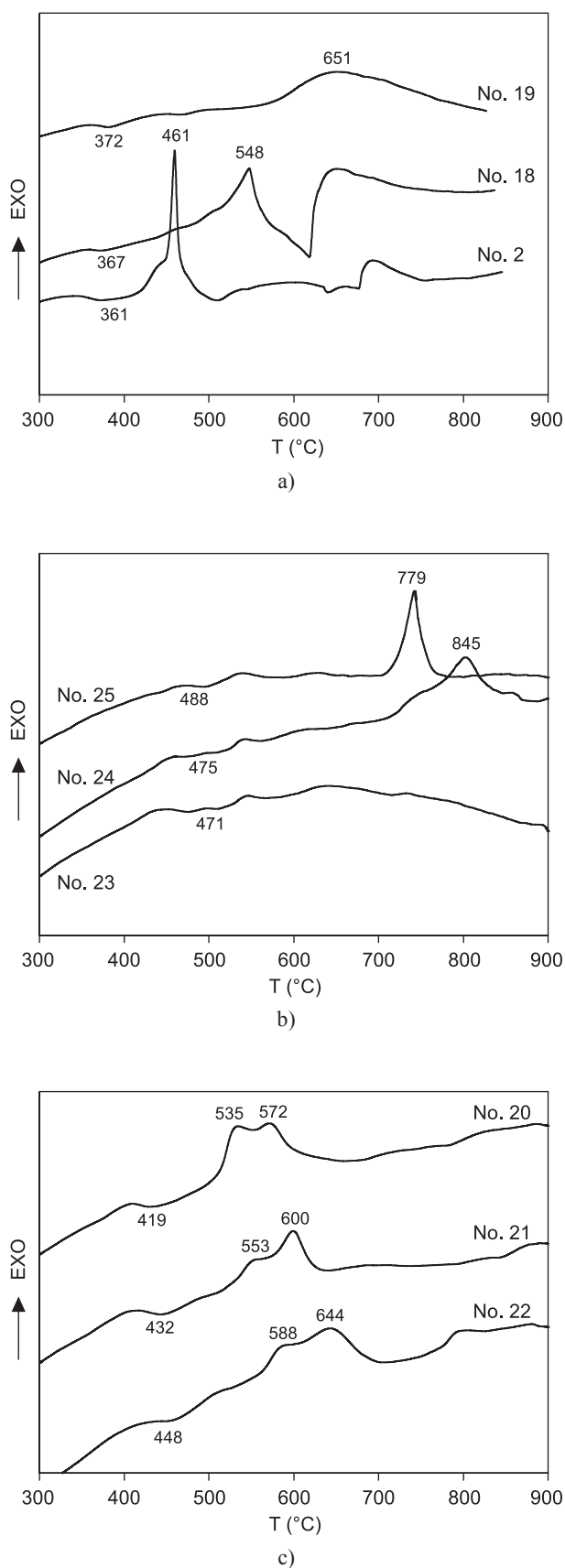


Figure 4. DTA curves of the glass samples: a) No. 2, 18, 19; b) No. 23, 24, 25; c) No. 20, 21, 22.

#### Density of the obtained glasses

The densities of the glasses discussed above are listed in Table 1. It can be seen that from point 19 to 18 and 2, when the amount of  $\text{Fe}_2\text{O}_3$  is fixed, the density of glass increases with  $\text{Li}_2\text{O}$ . A similar trend is also found in the cases when the amounts of  $\text{Fe}_2\text{O}_3$  are increased while the amount of  $\text{Li}_2\text{O}$  is fixed (No.25-24-23). The results suggest that both  $\text{Fe}_2\text{O}_3$  and  $\text{Li}_2\text{O}$  making the phosphate glass network more compact. The cross-linking effect of  $\text{Fe}_2\text{O}_3$  has been evidenced by the reduced crystallization tendency of glasses with increasing amounts of  $\text{Fe}_2\text{O}_3$  (see DTA results and Figure 4b). The addition of alkaline components to a glass generally creates non-bridging oxygens by breaking the chains/rings/3D closed network of the glass former. This is also true when more  $\text{Li}_2\text{O}$  is added into the phosphate glasses. However, due to the high electric field strength of  $\text{Li}^+$  ions, their aggregation effect could be dominant, contributing to the observed increase in the density of glasses. If the amount of  $\text{P}_2\text{O}_5$  is fixed (for example, point 20-22), the density of the glasses increases when  $\text{Li}_2\text{O}$  is replaced by  $\text{Fe}_2\text{O}_3$  [12]. This is mainly due to the fact that the latter oxide has a much larger molecular weight than the former. Among the above discussed samples, sample No.19 which has the lowest amount of  $\text{Fe}_2\text{O}_3$  has the smallest density; while sample No.23 containing the highest amount of  $\text{Fe}_2\text{O}_3$  has the largest density. The result indicates a relatively large contribution of  $\text{Fe}_2\text{O}_3$  to the density of glass as a whole.

#### Water attack resistance of the obtained glasses

The weight losses of different glasses after being boiled in water [13] are shown in Table 2. Comparisons of the weight losses of samples No. 2 and 18 as well as those of samples No.23, 24 and 25 lead to the conclusion that glasses with increasing amounts of  $\text{P}_2\text{O}_5$  are less resistant to water attack. The density measurement results have demonstrated that the glasses with higher amounts of  $\text{P}_2\text{O}_5$  have relatively loose structures [14], explaining their relatively poor chemical durability. The weight losses of samples No. 20-22 and 23-25 indicate substituting  $\text{P}_2\text{O}_5$  or  $\text{Li}_2\text{O}$  partially with  $\text{Fe}_2\text{O}_3$  could improve the chemical stability of the ternary phosphate glasses. In line with the DTA and density measurement results,  $\text{Fe}_2\text{O}_3$  has been found to strengthen the network of phosphate glasses. However, the glasses which have large amounts of  $\text{Li}_2\text{O}$  (such as No. 19, 18, 2) are generally less resistant to water attack, indicated by the large weight losses presented in Table 2. However, the weight loss of the ternary phosphate glass is not monotonically increased with the amount of  $\text{Li}_2\text{O}$ . On the one hand, as suggested by the density measurement results, when  $\text{P}_2\text{O}_5$  is partially replaced by  $\text{Li}_2\text{O}$ , the glass

Table 1. Density of lithium iron phosphate glasses with compositions inside the glass formation region.

Point in Figure 1	2	18	19	20	21	22	23	24	25
Molar ratios of components $\text{Li}_2\text{O}:\text{Fe}_2\text{O}_3:\text{P}_2\text{O}_5$	50:10:40	40:10:50	30:10:60	30:20:50	25:25:50	20:30:50	10:35:55	10:30:60	10:25:65
Density ( $\text{g}/\text{cm}^3$ )	2.5387	2.5285	2.4766	2.6553	2.7320	2.7601	2.8153	2.7390	2.6812

Table 2. Weight losses of lithium iron phosphate glasses after being boiled in water.

Point in Figure 1	2	18	19	20	21	22	23	24	25
Molar ratios of components $\text{Li}_2\text{O}:\text{Fe}_2\text{O}_3:\text{P}_2\text{O}_5$	50:10:40	40:10:50	30:10:60	30:20:50	25:25:50	20:30:50	10:35:55	10:30:60	10:25:65
Weight loss (%)	11.68	20.95	1.22	1.07	0.99	0.53	0.26	0.40	0.73

network becomes more compact due to the aggregation effect of  $\text{Li}^+$  ions. On the other hand, the inclusion of  $\text{Li}^+$  ions creates more non-bridging oxygens breaking the glass network. Meanwhile,  $\text{Li}^+$  ions have high mobility in water and are easily to be dissolved. The double-side effects of  $\text{Li}_2\text{O}$  on the glass network explain why the glass No.18 which has moderate  $\text{Li}_2\text{O}$  show the largest weight loss among the studied samples.

### CONCLUSION

The glass formation region of the  $\text{Li}_2\text{O}-\text{Fe}_2\text{O}_3-\text{P}_2\text{O}_5$  ternary system has been determined. Studies on the glasses with compositions inside the glass formation region show that both  $\text{Li}_2\text{O}$  and  $\text{Fe}_2\text{O}_3$  can increase the density of the ternary glass. It has been found that  $\text{Fe}_2\text{O}_3$  is beneficial for increasing the water attack resistance and reducing the crystallization tendency of the ternary glass. However, the increase in the amount of  $\text{Li}_2\text{O}$  has generally negative effects.

### Acknowledgment

*This work was financially supported by the opening projects foundation from State Key Laboratory of Crystal Material, Shandong University.*

### References

1. Majima M., Ujiie S., Yagasaki E., Koyama K., Inazawa S.: *J Power Sources* *101*, 53 (2001).
2. Wang H., Zhang W.D., Zhu L.Y., Chen M.C.: *Solid State Ionics* *178*, 131 (2007).
3. Padhi A.K., Najundaswamy K.S., Goodenough J.B.: *J. Electrochem. Soc.* *144*, 1188 (1997).
4. Yamada A., Chung S.C.: *J. Electrochem. Soc.* *148*, A224 (2001).
5. Ruffo R., Mari C.M., Morazzoni F., Rosciano F., Scotti R.: *Ionics* *13*, 287 (2007).
6. Fergus J.W.: *J. Power Sources* *195*, 939 (2010)
7. Hirose K., Tsuyoshi H., Benino Y., Komatsu T.: *Solid State Ionics* *178*, 801 (2007).
8. Gorkowska I., Jozwiak P., Garbarczyk J.E., Wasiucionek M., Julien C.M.: *J. Therm. Anal. Calorim.* *93*, 759 (2008).
9. Jozwiak P., Garbarczyk J.E., Wasiucionek M., Gorzkowska I., Gendron F., Mauger A., Julien C.M.: *Solid State Ionics* *179*, 46 (2008).
10. Jozwiak P., Garbarczyk J.E., Gendron F., Mauger A., Julien C.M.: *J. Non-Cryst. Solids* *354*, 1915 (2008).
11. Pakhomov G.B., Neverov S.L.: *Solid State Ionics* *119*, 235 (1999).
12. Mesko M.G., Day D.E.: *J. Nucl. Mater.* *273*, 27 (1999).
13. Reis S.T., Karabulut M., Day D.E.: *J. Non-Cryst. Solids* *292*, 150 (2001).
14. Garbarczyk J.E., Wasiucionek M., Jozwiak P., Tykarski L., Nowinski J.L.: *Solid State Ionics* *154*, 367 (2002).